JCTC Journal of Chemical Theory and Computation

Exploring the Reactivity Trends in the E2 and S_N2 Reactions of $X^- + CH_3CH_2Cl$ (X = F, Cl, Br, HO, HS, HSe, NH_2 PH_2, AsH_2, CH_3, SiH_3, and GeH_3)

Xiao-Peng Wu,[†,‡] Xiao-Ming Sun,[‡] Xi-Guang Wei,[‡] Yi Ren,*[,‡] Ning-Bew Wong,*[,†] and Wai-Kee Li[§]

Department of Biology and Chemistry, City University of Hong Kong, Kowloon, Hong Kong, College of Chemistry, Key Laboratory of Green Chemistry and Technology, Ministry of Education, and Key State Laboratory of Biotherapy, Sichuan University, Chengdu 610064, People's Republic of China, and Department of Chemistry, The Chinese University of Hong Kong, Shatin, N.T., Hong Kong

Received January 22, 2009

Abstract: The reactivity order of 12 anions toward ethyl chloride has been investigated by using the G2(+) method, and the competitive E2 and S_N2 reactions are discussed and compared. The reactions studied are $X^- + CH_3CH_2Cl \rightarrow HX + CH_2{=}CH_2 + Cl^-$ and $X^- + CH_3CH_2Cl \rightarrow CH_3CH_2X + Cl^-$, with X = F, Cl, Br, HO, HS, HSe, NH_2 PH_2, AsH_2, CH_3, SiH_3, and GeH_3. Our results indicate that there is no general and straightforward relationship between the overall barriers and the proton affinity (PA) of X^-; instead, discernible linear correlations only exist for the X's within the same group of the periodic table. Similar correlations are also found with the electronegativity of central atoms in X, deformation energy of the E2 transition state (TS), and the overall enthalpy of reaction. It is revealed that the electronegativity will significantly affect the barrier height, and a more electronegative X will stabilize the E2 and S_N2 transition states. Multiple linear regression analysis shows that there is a reasonable linear correlation between E2 (or S_N2) overall barriers and the linear combination of PA of X^- and electronegativity of the central atom.

1. Introduction

Base-induced bimolecular elimination (E2) and bimolecular nucleophilic substitution (S_N2) reactions are two fundamental organic reactions in synthesis. They play an important role in the development of modern mechanistic physical organic chemistry.[1] In many cases, E2 and S_N2 pathways are usually competitive processes. The S_N2/E2 competition in the gas phase and condensed phase has been exhaustively investigated experimentally[2−12] and theoretically[13−20] over the past 30 years, which helps us with a better understanding of the factors controlling the competition between them. For example, by direct detection of the neutral products, Jones et al.[2] found that elimination was preferred for the gas-phase reactions between the methoxide ion (CH_3O^-) and 1-bromopropane ($CH_3CH_2CH_2Br$). Their results in the gas phase contrast sharply with those in solution studies,[3] which show an overwhelming preference for S_N2. Although the neutral detection methods could provide useful information, their applications are restricted by experimental difficulties and limitations. Later, Gronert el al.[5−7] proposed a novel approach for analyzing the product mixtures to investigate the gas-phase S_N2/E2 competition. By using a double charged nucleophile (Nu) where the anionic site is nucleophilic and the other is unreactive, its reaction with alkyl halide will produce two charged species: a halide ion and an alkylated (S_N2 pathway) or a protonated (E2 pathway) nucleophile. In this way, two mechanisms can be identified. The reactions

* Corresponding author fax: +86-28-85412907 (Y.R.), +852-27887406 (N.-B.W.); e-mail: yiren57@hotmail.com (Y.R.), bhnbwong@cityu.edu.hk (N.-B.W.).

[†] University of Hong Kong.

[‡] Sichuan University.

[§] The Chinese University of Hong Kong.

10.1021/ct900041y CCC: $40.75
Published on Web 04/30/2009

of dialkyl ethers with bases have been the subject of several studies. In the early works by DePuy and Bierbaum,[8,9] the flowing afterglow (FA) technique was employed to study the gas-phase reactions of a series of dialkyl ethers with amide and hydroxide ions. It was observed that cyclic and acyclic ethers with β-hydrogens react rapidly in the gas phase with both NH_2^- and OH^- by elimination rather than substitution pathways due to ring-strain release and reaction exothermicity. In a different study,[10] DePuy et al. investigated the gas-phase E2/S_N2 competition by measuring the rate coefficients for the gas-phase reactions of alkyl chlorides and bromides with a set of nucleophiles, F^-, Cl^-, RO^- (R = H, CH_3, CF_3CH_2, $C_2F_5CH_2$), and RS^- (R = H and NH_2). On the basis of their obtained reactivity trends, it was found that Nus (F^- and RO^-) involving first-row elements are capable of undergoing both substitution and elimination, whereas the second-row Nus (e.g., HS^- and H_2NS^-) are mainly limited to substitution reactions. Moreover, RS^- induces elimination much less readily than does the RO^- even when the two anions have identical basicities.

In an early theoretical study, Yamabe et al.[13] studied the gas-phase E2 and S_N2 reactions of fluoride anion with fluoroethane by ab initio calculations at the level of HF/3-21G(+p). Comparison of the two competitive reaction pathways reveals that the mechanism of E2 reaction and the geometry of the E2 TS are completely different from those of the S_N2 reaction. Meanwhile, their Hartree−Fock calculations showed that the activation barrier of the E2 reaction is higher than that of the S_N2 reaction, which is in disagreement with the experimental results of Ridge and Beauchamp[12] on the $F^- + CH_3CH_2F$ system, where the E2 pathway is more favored in the gas phase. More recently, Bickelhaupt et al.[14] made an ab initio and DFT benchmark study on the E2 and S_N2 reactions of $X^- + CH_3CH_2X$ (X = F, Cl), indicating that the *anti*-E2 pathway dominates for $F^- + CH_3CH_2F$, and the backside S_N2 pathway is more favorable for $Cl^- + CH_3CH_2Cl$, while *syn*-E2 is the least favorable pathway in all cases, indicating that a fairly high level of theory is required in the studies on the S_N2 and E2 reactions. Gronert et al.[15−20] carried out a series of comprehensive theoretical studies on elimination reactions as well as S_N2 pathways with ab initio calculations. Using the G2+ approach, Gronert and co-workers[15] also studied the reaction of F^- with CH_3CH_2F and concluded that the E2 should dominate because its barrier is smaller and its pathway is less demanding entropically. At the level of MP4SDQ/6-31+G(d, p)/HF/6-31(+)G(d), Gronert et al.[16] investigated the reactions of F^- and PH_2^- with CH_3CH_2C1 and discussed the competition between S_N2 and E2 mechanisms for the first- and second-row nucleophiles. Their theoretical results indicated that the first-row Nus are well-suited for both S_N2 and E2 reactions, whereas second-row Nus with similar basicity are more confined to S_N2 reactions, which is consistent with the results of the aforementioned gas-phase experimental studies by DePuy et al.[10] The enhanced reactivity of fluoride anion could be rationalized by electron reorganization; that is, less electron density redistribution during either reaction will lead to a lower activation barrier. In another study, Gronert and co-workers evaluated the effect of methyl substitution on E2 and S_N2 mechanisms for the gas-phase reactions of F^- with $(CH_3)_2CHCl$ and $CH_3CH_2CH_2Cl$ at the MP2/6-31+G(d,p)//HF/6-31+G(d) level. A comparison of the activation barriers of the S_N2 and E2 reactions predicts that elimination will dominate in the reaction of propyl chloride.[17]

Recently, several studies have focused on a competitive reaction system, $ClO^- + CH_3CH_2Cl$ via E2 and S_N2 channels. By dual-level generalized transition state theory and statistical calculations based on high-level correlated electronic structure calculations using MP2 theory level and modified aug-cc-pVDZ basis set (MP2/ADZP), Hu and Truhlar[21] quantitatively evaluated the rate constants and deuterium kinetic isotope effects (KIEs) for the competing S_N2/E2 reactions of ClO^- with C_2H_5Cl or C_2D_5Cl in the gas phase. It was predicted that KIEs at room temperature were "normal" ($k_H/k_D = 3.1$) for the E2 reaction but "inverse" ($k_H/k_D = 0.6$) for the S_N2 reaction. Villano et al.[22] measured the overall reaction rate constants and KIEs for the gas-phase reactions of $RCl + ClO^-$ (R = CH_3, C_2H_5, iso-C_3H_7, and *tert*-C_4H_9) using a tandem flowing afterglow-selected ion flow tube (FA-SIFT) instrument. The experimental reaction efficiencies (10%)[23] and the KIEs ($k_H/k_D = 0.99 \pm 0.01$) for the reaction of ClO^- with C_2H_5Cl were shown to differ from the theoretical values (28% and 2.4) by Hu et al.,[21] suggesting that the S_N2 channel is more prominent in experiment than the calculated prediction. They proposed that nonstatistical dynamics or errors in the calculation of the individual KIE or in the branching ratios of the two channels could account for the discrepancies between experiment and theory, and additional studies were suggested to describe nucleophilic substitution and elimination reactions more accurately. To amend the shortage of the theoretical studies in the condensed phase, recently Pabis et al.[24] studied the KIEs on the two alternative reactions, S_N2 and E2, between ClO^- and C_2H_5Cl in water using B3LYP and M06-2X[25,26] functionals with the standard 6-31+G(d,p) basis set and the polarizable continuum solvent model (PCM).[27] The results show that the KIEs obtained using both DFT functionals are in qualitative agreement. It is worth noticing that this ^{18}O-KIE is a good indicator of different mechanism.

A Brønsted-type plot of log k_{nuc} versus pK_a constructed for a series of related Nus is often used to describe the relationship of basicity with nucleophilic character for the generalized acid−base reactions, for example, S_N2, and also base-induced E2 reactions. As mentioned above, Gronert et al.[16] pointed out that there might be significantly different reactivity for the nucleophiles (or base) with similar basicity, implying that the linear Brønsted-type plot does not hold for all cases and is only valid for selective Nus. There are several theoretical studies treating the reactivity order of Nus in the S_N2 reactions. Radom et al.[28,29] reported G2(+) studies on the reactions of halide anions with methyl halides, giving the nucleophilic order of halides toward methyl halides, $F^- > Cl^- > Br^- > I^-$; Bickelhaupt et al.[30] also carried out a study on the nucleophilicity of halide anions using relativistic density functional theory (DFT) and found that the S_N2 barriers would increase along the nucleophiles F^-, Cl^-, Br^-, and I^-. Lee et al.[31] made ab initio studies on the S_N2 identity exchange reactions $RCH_2X + X^- \rightarrow X^- + RCH_2X$ for R =

CH_2CH with X = H, NH_2, OH, F, PH_2, SH, and Cl, and for R = CH_3 and CH≡C with X = Cl at the HF and MP2 levels of theory using the 6-31++G(d,p) basis set. They concluded that the activation barriers, and major structural changes, $\Delta d^{\ddagger}$(C−X), in the activation process are closely related to the electronegativity of the R and X groups (we will use the abbreviation EN for electronegativity from now on), and a stronger EN of R and/or X leads to less electronic as well as structural reorganization in the activation, which in turn would lower the energy barriers at both the HF and the MP2 levels. Uggerud,[32] using G2 calculations, investigated 18 S_N2 reactions, including $X^- + CH_3X \rightarrow XCH_3 + X^-$ and $XH + CH_3XH^+ \rightarrow {}^+HXCH_3 + XH$ (X = F, Cl, Br, OH, SH, SeH, NH_2, PH_2, and AsH_2), and analyzed the systematic periodic trends of intrinsic reactivity, finding that the barrier heights decrease on going from left to right of each row in the periodic table, and the basicity and nucleophilicity will be equivalent only in the strongly exothermic reactions.

Despite the importance of E2 reactions in organic synthesis, there has been less effort put on the reactivity in the base-induced E2 reactions than on S_N2 reactions until now. In the present work, G2(+) calculations are reported for a series of anionic E2 reactions toward ethyl chloride with 12 attacking atoms from groups 14−17 of the periodic table (eq 1). The corresponding competitive S_N2 reactions (eq 2) are also discussed for the sake of comparing the reactivity with that of the E2 reactions.

$$X^- + CH_3CH_2Cl \rightarrow CH_2{=}CH_2 + XH + Cl^- \quad (1)$$

$$X^- + CH_3CH_2Cl \rightarrow CH_3CH_2X + Cl^- \quad (X = F, Cl, Br, HO, SH, SeH, NH_2, PH_2, AsH_2, CH_3, SiH_3, \text{and } GeH_3) \quad (2)$$

In this work, our objectives are to find systematic periodic trends in reactivity for the base-induced E2 reactions and to provide a reasonable and consistent set of ab inito barrier height data. We will focus on the relationship between basicity and reactivity and make an extensive comparison between the E2 and the S_N2 reactions.

2. Computational Methods

Previous studies have proved that the high-level G2(+) theory, introduced by Radom and co-workers,[33] treated anions better with the added diffuse functions on non-hydrogen atoms and is able to provide reliable data for the anionic S_N2 and E2 reactions.[28,29,33−37] Therefore, the G2(+) theory was employed in the present study. We note here that the original G2(+) procedure corrects the zero-point vibrational energy using HF/6-31+G(d) frequencies, scaled by 0.8929. For some of the species studied here, especially some TSs, the HF/6-31+G(d) and MP2(fc)/6-31+G(d) structures are considerably different. Hence, for all of the values reported below, the zero-point energy was corrected at the MP2(fc)/6-31+G(d) level, using the recommended scaling factor of 0.98.[38] We also note here that using MP2/6-31+G(d) frequencies, in place of the HF/6-31+G(d) frequencies, has virtually no effect on the calculated proton affinities for all of the anions. Charges were calculated by the natural population analysis (NPA)[39] at the MP2(fc)/6-311+G(3df,2p) level on the MP2(fc)/6-31+G(d) geometries.

Table 1. Proton Affinity (PA) and Ethyl Cation Affinity (ECA) and Available Methyl Cation Affinity of Anions (in kJ mol^{-1})

X^-	G2(+) PA	G3 (MP2) PA[a]	exp. PA[b]	G2(+) ECA	G2 MCA[d]	exp. MCA[b]
F^-	1550.7	1553.9	1554.0	925.7	1078	1080
Cl^-	1397.5	1390.3	1395.0	791.4	950	952
Br^-	1354.5	1358.5	1353.5 ± 0.42	755.4	916	916
HO^-	1631.3	1632.2	1633.0	1000.6	1153	1159
HS^-	1472.1	1464.8	1468.0 ± 12.	869.6	1034	1033
HSe^-	1429.1	1433.4	1428.8 ± 2.9	831.9	999	
NH_2^-	1688.8	1686.2	1687.8 ±0.42	1067.5	1225	1234
PH_2^-	1539.0	1530.5	1536.0[c]	956.9	1124	1116
AsH_2^-	1500.6	1504.6	1496.0 ± 8.8	916.0	1085	
CH_3^-	1746.6	1746.0	1743.5 ± 2.9	1148.1		
SiH_3^-	1562.8	1557.3	1564.0 ± 8.8	999.8		
GeH_3^-	1517.7	1518.4	1501.0 ± 8.8	942.1		

[a] From ref 48. [b] From ref 44. [c] From ref 46. [d] From ref 32.

The geometrical characteristics of the TSs are described by the Pauling bond order, $n^{\ddagger}$, calculated according to eq 3, where r and $r^{\ddagger}$ are the bond lengths at the reactant (CH_3CH_2Cl) or the products (HX, CH_3CH_2X, and $CH_2{=}CH_2$), and at the TSs, respectively. The constant a is usually set to 0.26 or 0.3 Å. However, it has been found that a proportionality constant of a = 0.6 Å is more appropriate for the case where the bond in question has a bond order less than 1.[40−42] Based on the suggestions in the literature, a = 0.6 Å is adopted here for the calculations of bond order $n^{\ddagger}(X{-}H^{\beta})$, $n^{\ddagger}(C^{\beta}{-}H^{\beta})$, and $n^{\ddagger}(C^{\alpha}{-}Cl)$, while a = 0.3 Å is opted for $n^{\ddagger}(C^{\alpha}{-}C^{\beta})$.

$$n^{\ddagger} = \exp[(r - r^{\ddagger})/a] \quad (3)$$

Throughout this Article, all distances are in angstroms (Å) and all angles are in degrees (°), while energies are in kJ mol^{-1}. The overall barriers of the two series of reactions relative to free reactants are denoted as $\Delta H^{\ddagger}$(E2) for E2, and $\Delta H^{\ddagger}(S_N2)$ for S_N2, respectively. The MP2/6-31+G(d) optimized geometries and G2(+) energies of all reactants, products, and TSs involved in E2 (eq 1) and S_N2 reactions (eq 2) are given in the Supporting Information. The Gaussian 03 program package[43] was used in all calculations.

3. Results and Discussion

3.1. Proton Affinities and Ethyl Cation Affinity. The gas-phase basicity of an anion is usually measured in terms of its proton affinity (PA), that is, the negative of the enthalpy change for a gas-phase reaction like eq 4; the higher is the proton affinity, the stronger is the base and the weaker is the conjugate acid in the gas phase.

$$X^- + H^+ \rightarrow HX \quad (4)$$

The calculated and experimental PAs[44−46] of the 12 simple anionic bases given in eqs 1 and 2 are listed in Table 1. Inspection of the results in Table 1 shows that theoretical values generally compare well with their experimental counterparts, and most of them are within the so-called chemical accuracy (roughly 10 kJ mol^{-1}). The most pronounced discrepancy occurs in GeH_3^-, for which the G2(+)

Scheme 1. E2 and S_N2 Pathways for $X^- + CH_3CH_2Cl$

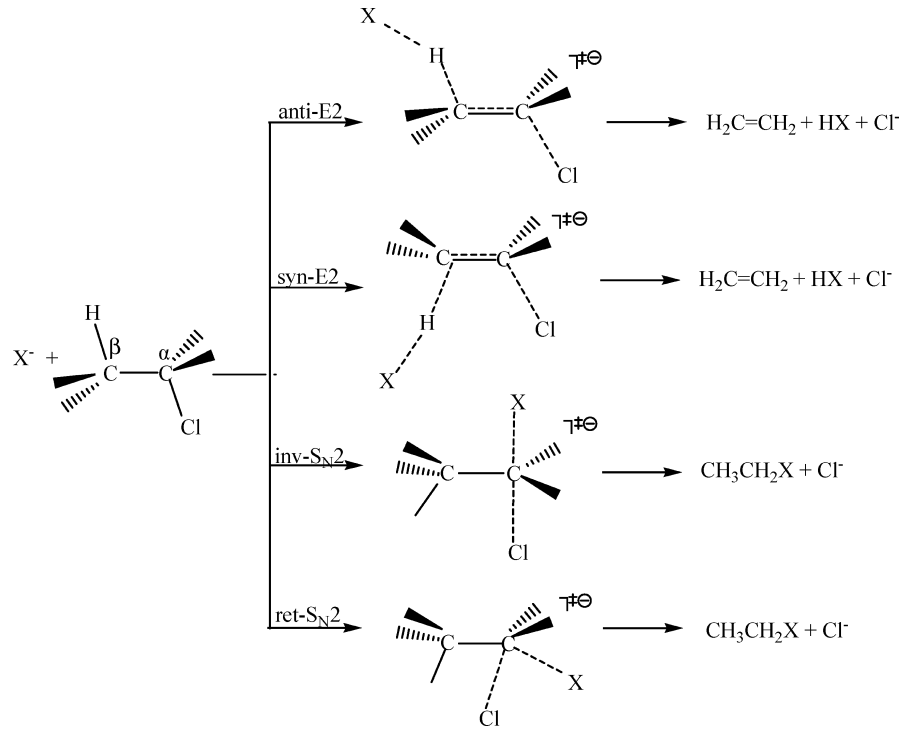

result is about 17 kJ mol^{-1} higher than the experimental value obtained by Decouzon et al.[45] by Fourier transform-ion cyclotron resonance (FT-ICR) spectrometry. Mayer et al.[47] and Bartmess et al.[48] also got similar results for the PA value of GeH_3^- by G2 and G3(MP2) theoretical methods, respectively.

Analogous to the methyl cation affinity (MCA) involved in the S_N2 reactions with CH_3Cl, ethyl cation affinity (ECA, defined as the enthalpy of the reaction $CH_3CH_2X \rightarrow CH_3CH_2^+ + X^-$) of the 12 anions was also calculated. Agreeing with numerous previous calculations,[49−55] the present study at the G2(+) level also demonstrates that, for $C_2H_5^+$, the structure with C_{2v} symmetry and a three-center two-electron bond with the $^1A_1$ ground electronic state is the global minimum on the potential-energy surface (PES). This result was proved recently by the highly sensitive technique of single photon IR photodissociation (IRPD) spectroscopy.[56] The calculated ECA values are found to be well correlated ($R^2 = 0.996$) with the available theoretical MCA results by the G2 method.[32]

3.2. Geometries of S_N2 and E2 Transition States. There are two possible pathways, *anti*- and *syn*-elimination, for the base-induced E2 reactions (see Scheme 1). Several previous studies[14,16] compared the energies for the *anti*- and *syn*-E2 TSs and showed that the former pathway has TSs much lower energy than the latter. For example, the *syn*-E2 TS for the F^--induced elimination of CH_3CH_2Cl lies 53.1 kJ mol^{-1} above the corresponding *anti*-E2 TS at the MP4/SDQ/6-31+G(d,p)//HF/6-31+G(d) level.[16]

For the anionic S_N2 reactions, there are also two possible pathways, back-side S_N2 with inversion of configuration and front-side S_N2 with retention of configuration (inv-, or ret-S_N2; see Scheme 1). Previous studies by Glukhovtsev et al.[28,33] on the gas-phase identity S_N2 reactions of halide anions and methyl halides, $X^- + CH_3X$, showed that the calculated G2(+) overall gas-phase barriers for the retention pathway are substantially higher than the corresponding values for back-side attack with inversion of configuration by more than 164.9 kJ mol^{-1}. More recently, Bickelhaupt et al.[33] explored the PESs of the back-side as well as the front-side S_N2 reactions of $X^- + CH_3Y$, with X, Y = F, Cl, Br, and I, using relativistic DFT, and concluded that the front-side S_N2 barriers in all cases were much higher in energy (ca. 160 kJ mol^{-1}), due to a more severe steric repulsion as a result of the proximity between the Nu and the leaving group.

In the present study, the reaction of CH_3CH_2Cl with one representative base, F^-, is used to check the G2(+) energy difference between the back-side and front-side S_N2 TSs with its competitive *anti*- and *syn*-E2 TSs. Figure 1 presents the structures of these two pairs of TSs and their G2(+) energies relative to separated reactants, F^- and CH_3CH_2Cl. The calculated G2(+) energy of the *syn*-E2-TS is higher than that of the *anti*-E2-TS by 45.0 kJ mol^{-1}, signifying that the *anti*-elimination pathway is energetically favorable in the E2 reaction of F^- with CH_3CH_2Cl. The calculated overall G2(+) barrier for the back-side S_N2 reaction is much lower (by 169.2 kJ mol^{-1}) than that of the front-side S_N2 reaction of F^- with CH_3CH_2Cl, indicating that the inv-S_N2 pathway is much more favorable than the retention one. So, we will only focus on the back-side S_N2 and *anti*-E2 TS structures in the following discussion.

The key TS structural parameters for the back-side S_N2 transition states are the distance between the attacking atom and the central carbon, $X\cdots C^\alpha$, and the distance between the central carbon atom and the leaving chloride ion, $C^\alpha\cdots Cl$. These distances can be better assessed by their bond orders $n^\ddagger(X-C^\alpha)$ and $n^\ddagger(C^\alpha-Cl)$ (see Table 2). It is found that the

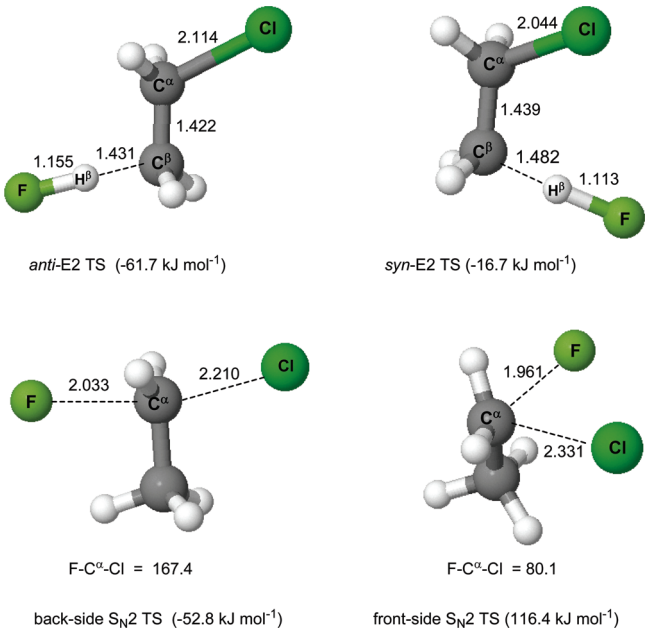

Figure 1. MP2/6-31+G(d) optimized structures for the *anti* and *syn* E2 TSs, back-side and front-side S_N2 TSs of ethyl chloride with fluoride ion, in which the bond lengths and angles are in angstroms and degrees, respectively. The numbers in parentheses are the G2(+) energies relative to the separated reactants, CH_3CH_2Cl and F^-.

Table 2. Selected Geometrical Parameters (in Normal Font) and the Bond Order, $\Delta n^{\ddagger}$(in Bold Font), in the S_N2 TS Structures $[X\cdots Et\cdots Cl]^{-\ddagger}$

X^-	$r(X-C^{\alpha})$	$n^{\ddagger}(X-C^{\alpha})$	$r(C^{\alpha}-Cl)$	$n^{\ddagger}(C^{\alpha}-Cl)$
F^-	2.033	**0.358**	2.210	**0.499**
Cl^-	2.354	**0.392**	2.381	**0.375**
Br^-	2.456	**0.440**	2.404	**0.361**
HO^-	2.202	**0.279**	2.155	**0.547**
HS^-	2.540	**0.304**	2.264	**0.456**
HSe^-	2.610	**0.339**	2.253	**0.465**
NH_2^-	2.384	**0.218**	2.103	**0.597**
PH_2^-	2.745	**0.230**	2.191	**0.515**
AsH_2^-	2.791	**0.251**	2.165	**0.538**
CH_3^-	2.647	**0.155**	2.060	**0.641**
SiH_3^-	2.808	**0.216**	2.190	**0.516**
GeH_3^-	2.730	**0.266**	2.180	**0.525**

S_N2 TS structures have decreasing $n^{\ddagger}(X-C^{\alpha})$ values on going from left to right of a given row in the periodic table and increasing when going down a group, showing that there is an earlier TS for the Nu with stronger basicity. Unexpectedly, the $C^{\alpha}-Cl$ distances for the S_N2 TSs do not increase monotonically from top to bottom for the groups 14−16 Nus with decreasing PA values. For example, the $C^{\alpha}-Cl$ distance in the S_N2 TS $[HS\cdots Et\cdots Cl]^{-\ddagger}$ is slightly longer than that in the $[HSe\cdots Et\cdots Cl]^{-\ddagger}$. This trend is also observed in groups 14 and 15. The magnitude of geometrical deformation of TSs can be described by their deformation energy, ΔH_{def}, defined as the enthalpy change accompanying the transformation from equilibrium reactant structures to the corresponding TS, which is also called "activation strain" by Bickelhaupt. Obviously, higher deformation energy for the S_N2 reaction arises mainly from the more cleaved $C^{\alpha}-Cl$ bond in the TS, that is, the smaller $n^{\ddagger}(C^{\alpha}-Cl)$ value, which is supported by the good linear correlation ($R^2 = 0.992$) for the plot of $\Delta H_{def}(S_N2)$ against $n^{\ddagger}(C^{\alpha}-Cl)$.

For the E2 reactions, the main geometrical character of TSs can be described by $n^{\ddagger}(X-H^{\beta})$, $n^{\ddagger}(H^{\beta}-C^{\beta})$, $n^{\ddagger}(C^{\alpha}-C^{\beta})$, and $n^{\ddagger}(C^{\alpha}-Cl)$ (see Table 3), in which the elongation of $C^{\beta}-H^{\beta}$ and $C^{\alpha}-Cl$ bonds will significantly contribute to the deformation energy of E2 TS, and the smaller sum of $n^{\ddagger}(C^{\beta}-H^{\beta})$ and $n^{\ddagger}(C^{\alpha}-Cl)$ will result in a large $\Delta H_{def}(E2)$ value, leading to a reasonable correlation ($R^2 = 0.953$) for $n^{\ddagger}(C^{\beta}-H^{\beta}) + n^{\ddagger}(C^{\alpha}-Cl)$ against $\Delta H_{def}(E2)$. Data in Table 3 show that there are smaller $n^{\ddagger}(C^{\alpha}-C^{\beta})$ and larger $n^{\ddagger}(C^{\alpha}-Cl)$ values for the first-row bases (X= CH_3, NH_2, HO, and F) with stronger basicity. When the weaker bases, such as HSe^-, Cl^-, and Br^-, attack the H^{β} on the substrate, there are more product-like characteristics, as evidenced by the larger $n^{\ddagger}(C^{\alpha}-C^{\beta})$ and smaller $n^{\ddagger}(C^{\alpha}-Cl)$ values in those E2 TSs. In fact, the reasonable correlations existing for PA versus $n^{\ddagger}(C^{\alpha}-C^{\beta})$ ($R^2 = 0.963$) and versus $n^{\ddagger}(C^{\alpha}-Cl)$ ($R^2 = 0.957$) indicate a more product-like TS for the weaker bases.

3.3. The Barrier Heights for the S_N2 and E2 Reactions. It is well-known that the PESs for both of the S_N2 and E2 reactions have the shape of a double well, as shown in Scheme 2. The first step in the present study involves the initial exothermic formation of a reactant ion−molecule complex, $X^-\cdots CH_3CH_2Cl$. This complex is predestined to react further via a favorable back-side S_N2 or *anti*-E2 pathway. The reaction then proceeds via the S_N2 or *anti*-E2 TS, yielding the product complex (PC) $Cl^-\cdots CH_3CH_2X$ for the S_N2 pathway or $HX\cdots CH_2{=}CH_2\cdots Cl^-$ for the E2 pathway. These complexes can decompose into the products $Cl^- + CH_3CH_2X$ or $CH_2{=}CH_2 + HX + Cl^-$, in which the leaving group Cl^- and the conjugate acid HX can form a stable complex as the most stable products in the E2 pathway. Nibbering previously pointed out that the overall barrier, $\Delta H^{\ddagger}$, is decisive for the rate of chemical reactions in the gas phase, particularly if they occur under low-pressure conditions in which the reacting system is (in good approximation) thermally isolated.[57,58] This is the reason why we only discuss the overall barriers in the following discussion.

The G2(+) overall barriers for the back-side S_N2 and *anti*-E2 reactions with CH_3CH_2Cl, $\Delta H^{\ddagger}(S_N2)$, and $\Delta H^{\ddagger}(E2)$ are collected in Table 4. Bickelhaupt and his co-worker[30] found that the sequence given by $\Delta H^{\ddagger}$ in the S_N2 reactions of halides with methyl halides follows the decreasing order $I^- > Br^- > Cl^- > F^-$; that is, the reactivity order of halide anion decreases from top to bottom in group 17. This trend is also observed in the present S_N2 and E2 reactions of ethyl chloride; that is, the $\Delta H^{\ddagger}(S_N2)$ and $\Delta H^{\ddagger}(E2)$ values always increase within each group as we go down the periodic table. Our calculation results are in accord with the existing experimental data. For example, Bierbaum et al.[59] measured the rate coefficients for the substitution reactions of a series of anions toward CH_3I by using FA-SIFT techniques and reported the following reactivity order: $F^- > Cl^- > Br^-$ and $HO^- > HS^-$; Anderson et al.[60] investigated the gas PH_2^- reactions with a series of neutral substrates including CH_3Y (Y = Cl, Br, and I) using the

Table 3. Selected Geometrical Parameters (in Normal Font) and the Bond Order, $\Delta n^{\ddagger}$(in Bold Font), in the E2 TS Structures $[X\cdots H^{\beta}\cdots CH_2CH_2\cdots Cl]^{-\ddagger}$

X^-	$r(X-H^{\beta})$	$n^{\ddagger}(X-H^{\beta})$	$r(C^{\beta}-H^{\beta})$	$n^{\ddagger}(C^{\beta}-H^{\beta})$	$r(C^{\alpha}-C^{\beta})$	$n^{\ddagger}(C^{\alpha}-C^{\beta})$	$r(C^{\alpha}-Cl)$	$n^{\ddagger}(C^{\alpha}-Cl)$
F^-	1.155	**0.700**	1.431	**0.572**	1.422	**1.368**	2.114	**0.586**
Cl^-	1.514	**0.678**	1.494	**0.515**	1.378	**1.584**	2.489	**0.313**
Br^-	1.636	**0.717**	1.546	**0.472**	1.369	**1.632**	2.644	**0.242**
HO^-	1.297	**0.581**	1.363	**0.641**	1.453	**1.234**	1.975	**0.738**
HS^-	1.635	**0.612**	1.445	**0.559**	1.396	**1.492**	2.306	**0.425**
HSe^-	1.738	**0.649**	1.463	**0.542**	1.386	**1.542**	2.421	**0.351**
NH_2^-	1.444	**0.491**	1.325	**0.683**	1.46	**1.205**	1.938	**0.785**
PH_2^-	1.795	**0.530**	1.399	**0.604**	1.411	**1.419**	2.204	**0.504**
AsH_2^-	1.864	**0.577**	1.398	**0.605**	1.402	**1.462**	2.291	**0.436**
CH_3^-	1.642	**0.399**	1.298	**0.714**	1.461	**1.201**	1.93	**0.796**
SiH_3^-	1.903	**0.496**	1.399	**0.604**	1.413	**1.410**	2.193	**0.513**
GeH_3^-	1.895	**0.562**	1.411	**0.592**	1.402	**1.462**	2.28	**0.444**

Scheme 2. Schematic Potential Energy Diagrams for the Gas-Phase E2 and S_N2 Reactions, in Which the Plain Line Is for Negative Overall Barrier ($\Delta H_1^{\ddagger}$) and the Dashed Line Is for Positive Overall Barrier ($\Delta H_2^{\ddagger}$)

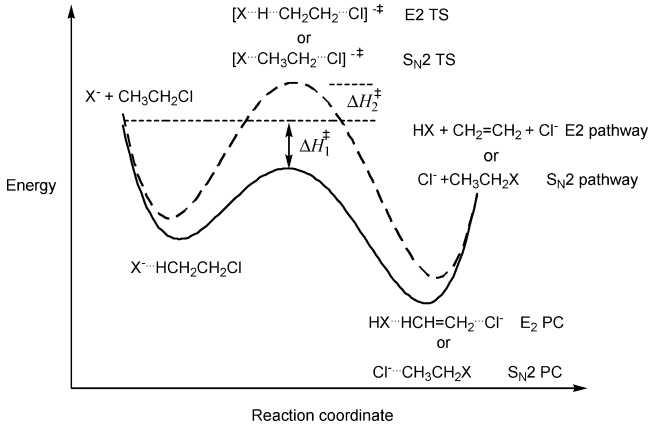

FA technique. These reactions were compared to those for the reactions of NH_2^-. Many similarities exist between the reactions of phosphide and those of amide, but the former reacts much less efficiently than the latter.

The overall barriers in Table 4 show that all of the S_N2 and E2 TSs for the four first-row bases have energies ranging from 36.3 to 63.5 kJ mol^{-1} below that of the separated reactants. The lower overall barriers are consistent with the higher complexation energies between X^- with higher PA values and CH_3CH_2Cl. For example, the G2(+) complexation enthalpy for the complex formed between F^- and CH_3CH_2Cl, $F^-\cdots CH_3CH_2Cl$, is -75.0 kJ mol^{-1} with respect to the separated reactants, leading to the overall barrier, $\Delta H^{\ddagger}(S_N2) = -52.8$ kJ mol^{-1} and $\Delta H^{\ddagger}(E2) = -61.7$ kJ mol^{-1}, much lower than the previous values of -28.0 and -23.8 kJ mol^{-1}, respectively, reported by Gronert et al.,[16] calculated at the MP4SDQ/6-31+G(d,p)//HF/6-31+G(d) level. A similar situation is also found in S_N2 TS $[H_2P\cdots Et\cdots Cl]^{-\ddagger}$, in which the G2(+) $\Delta H^{\ddagger}(S_N2)$ value is -6.1 kJ mol^{-1}.

The $\Delta H^{\ddagger}$ sequences for the S_N2 reactions show the following decreasing order:

$$HO < F < NH_2 < CH_3 < PH_2 < HS < AsH_2 \approx SiH_3 < GeH_3 < HSe < Cl < Br$$

The above order holds in most cases for the corresponding E2 reactions, but there are some deviations:

$$HO < F < NH_2 < CH_3 < PH_2 < HS < SiH_3 < AsH_2 < Cl < GeH_3 < HSe < Br$$

These two trends appear to be related to the reactivity of these anions toward ethyl chloride, which match the available experimental data.[10,59,60] It is worth noting that the differences of the S_N2 or E2 barriers involving the Nus (or bases) of similar basicity could be considerable. Moreover, the weaker base may show higher reactivity than the stronger one. For example, the PA values of HO^- and CH_3^- are 1631.3 and 1746.6 kJ mol^{-1}, respectively, but the calculated $\Delta H^{\ddagger}(S_N2)$ and $\Delta H^{\ddagger}(E2)$ values are -56.8 and -63.5 kJ mol^{-1} for HO^-, and -43.4 and -36.3 kJ mol^{-1} for CH_3^-, indicating that (1) CH_3^- has much lower reactivity than HO^- in both S_N2 and E2 reactions; (2) with hydroxide anion as the Nu, the elimination is more favorable than the substitution, but the two processes should be competitive; and (3) CH_3^- has preference for the back-side S_N2 pathway. These results imply that there are other factors for determining the reactivity of the Nu in the S_N2 or E2 reactivity in addition to its basicity.

Even though the enhanced reactivity of hydroxide anion could be explained by the hard and soft acids and bases (HSAB) principle, here the idea of electron reorganization is used to rationalize its stronger reactivity in the S_N2 and E2 reactions. In the S_N2 reaction of HO^- with CH_3CH_2Cl, the net charge on the HO moiety decreases from -1.00e to -0.33e (in S_N2 product CH_3CH_2OH). The change of population is much smaller than that in the S_N2 reaction of CH_3^- with CH_3CH_2Cl, in which the electron population on the CH_3 moiety shifts from 10.00e to 8.99e in going from reactant CH_3 to product $CH_3CH_2CH_3$, implying that much more electron on the HO will be retained than that on the CH_3 moiety in the product when S_N2 reaction occurs, which in turn will lead to a much lower S_N2 barrier for the reaction of HO^- with CH_3CH_2Cl.

This rationalization can be extended to the E2 reactions. When HO^- initiates the proton transfer of the *anti*-E2 pathway, the electron density on the HO^- moiety changes only from -1.00e to -0.47e in the product H_2O. In contrast, the E2 reaction of CH_3^- with CH_3CH_2Cl results in much more change of net charge, and the population on the CH_3 moiety shifts from 18.00e to 16.79e, leading to a significant

Table 4. Calculated G2(+) Reaction Barriers Relative to the Separated Reactants, $\Delta H^{\ddagger}$, Deformation Energies, ΔH_{def}, and Actual Interaction, ΔH_{int}, between the Deformed Reactants in the TS, and Total Reaction Enthalpy Changes, ΔH, for the Gas-Phase Reactions $X^- + CH_3CH_2Cl$[a]

X^-	$\Delta H^{\ddagger}(S_N2)$	$\Delta H^{\ddagger}(E2)$	$\Delta H_{def}(S_N2)$	$\Delta H_{def}(E2)$	$\Delta H_{int}(S_N2)$	$\Delta H_{int}(E2)$	$\Delta H(S_N2)$	$\Delta H(E2)$
F^-	−52.8	−61.7	87.8	146.4	−140.6	−208.1	−134.3	−80.8
Cl^-	18.1	61.3	140.2	262.3	−122.1	−201.0	0.0	72.3
Br^-	35.0	93.5	148.0	312.2	−113.0	−218.7	36.0	115.3
HO^-	−56.8	−63.5	68.9	88.1	−125.7	−151.6	−209.2	−161.4
HS^-	2.7	45.6	104.0	201.4	−101.3	−155.8	−78.2	−2.2
HSe^-	17.4	71.9	102.0	237.0	−84.5	−165.1	−40.5	40.7
NH_2^-	−50.3	−50.5	54.0	108.5	−104.3	−158.9	−276.1	−219.0
PH_2^-	−6.1	35.3	80.7	162.0	−86.8	−126.7	−165.5	−69.1
AsH_2^-	5.1	54.6	73.5	182.2	−68.4	−127.6	−124.6	−30.7
CH_3^-	−43.4	−36.3	40.4	57.4	−83.8	−93.7	−356.7	−276.7
SiH_3^-	5.2	52.3	83.4	167.5	−78.2	−115.2	−208.4	−92.9
GeH_3^-	16.8	67.7	80.7	193.6	−63.9	−125.9	−150.7	−47.8

[a] All energies are in kJ mol^{-1}.

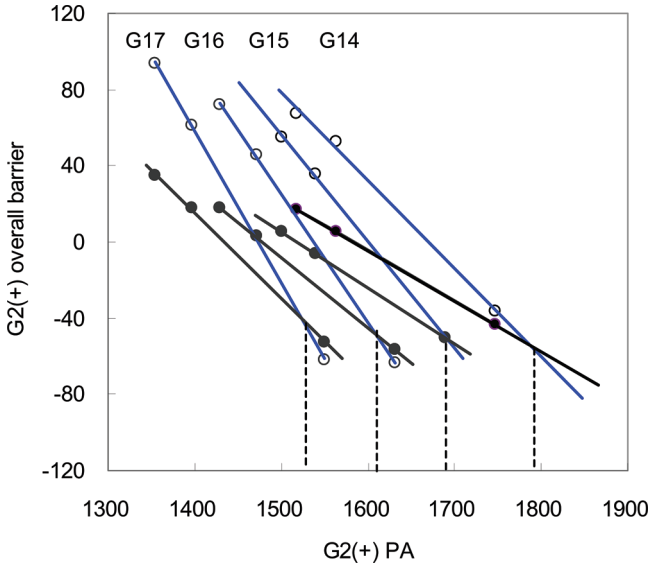

Figure 2. Plot of the G2(+) overall barrier (kJ mol^{-1}) vs the PAs (kJ mol^{-1}) along each column of the peordic table for *anti*-E2 reactions (blue line) and for back-side S_N2 reactions (black line).

electron reorganization and higher E2 barrier in the reaction of CH_3^- with ethyl chloride.

3.4. Correlation of E2 and S_N2 Barrier Height with PA and EN. Figure 2 shows the relation between the overall barrier for E2 reactions, $\Delta H^{\ddagger}(E2)$, and PA for various groups. It can be inferred from this figure that there is no general and straightforward relationship between $\Delta H^{\ddagger}(E2)$ and PA for all of the bases. Instead, there is an excellent linear relationship ($R^2 \approx 1.00$) within each column of the periodic table (see Figure 2). Similar trends occur for the corresponding S_N2 reactions (see also Figure 2).

In the early study of identity proton transfer reaction between simple hydrides ($AH + A^- \rightarrow A^- + AH$), Gronert[61] found a stronger correlation between the EN of central atom in A and the barrier to the proton transfer. He interpreted these results in terms of a model where the TS was dominated by the triple ion valence bond resonance configuration, $[A\cdots H\cdots A]^{-\ddagger} \leftrightarrow [A^-H^+A^-]^{\ddagger}$, where the transferring proton and base carried full charges. Obviously, this resonance form would be more stable when A is highly electronegative. The stabilization of TSs by resonance also seems to be applicable in the present S_N2 and E2 reactions. In the E2 reactions of CH_3CH_2Cl, proton transfer still takes place, and this transfer is accompanied by the leaving of a chloride ion. In the S_N2 reaction, the TS structure can be viewed as a resonance form similar to that in the proton transfer reaction. So there may be some type of relationship between the EN of attacking atom and the overall barriers. Here, the revised EN scales V_x (eq 5), suggested by Luo and Benson,[62] for the 12 attacking atoms covering groups 14−17 of the periodic table are used to correlate with the overall barriers of S_N2 and E2, where n_x is the number of valence electrons, and r_x is the covalent radius from ref 63:

$$V_x = n_x/r_x \quad (5)$$

The stabilization of the TS by more electronegative Nus can also be understood in terms of the bonding and, especially, the nonbonding orbital in the three-center four-electron picture of these species, which has been discussed in detail by Pierrefixe et al.[64−66] The occupied nonbonding MO has high amplitudes on the terminal groups (nucleophile and leaving group) and will be stabilized if these groups become more electronegative.

As in the case of PA, there are also good linear correlations ($R^2 = 0.99-1.00$) between EN and $\Delta H^{\ddagger}(E2)$ or $\Delta H^{\ddagger}(S_N2)$ for every column in the periodic table. Because both PA and EN are important for determining the E2 and S_N2 barriers, we should correlate the overall barrier with both PA and EN. We report here a two-parameter treatment of our results for all E2 (eq 1) or S_N2 reactions (eq 2) by multiple linear regression analysis. The results provide reasonable correlations (see eqs 6 and 7), indicating that it is possible to approximately predict the S_N2 and E2 overall barriers for normal Nu toward ethyl chloride on the basis only of the PA value of Nu and the EN value of the attacking atom. For example, the predicted values by using eqs 6 and 7 for the reaction of CH_3O^- and CH_3CH_2Cl are $\Delta H^{\ddagger}(E2) = -46.9$ kJ mol^{-1}, and $\Delta H^{\ddagger}(S_N2) = -51.4$ kJ mol^{-1}, which are very close to the calculated G2(+) ones, −48.3 and −50.7 kJ mol^{-1}. Using eq 5, the covalent radius of oxygen is 0.73 Å.[63]

$$\Delta H^{\ddagger}(E2) = -0.38PA - 17.69EN + 713.00 \; (R^2 = 0.986, n = 12) \quad (6)$$

$$\Delta H^{\ddagger}(S_N2) = -0.23PA - 8.89EN + 389.54 \; (R^2 = 0.974, n = 12) \quad (7)$$

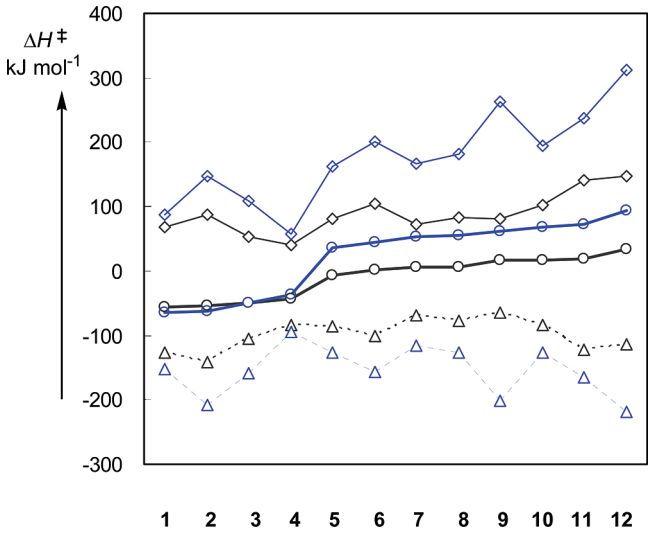

Figure 3. Variations of X^- with deformation energy (plain line), interaction between the deformed reactants (dashed line), and overall barrier (bold line) for the S_N2 (black line, X = 1, HO; 2, F; 3, NH_2; 4, CH_3; 5, PH_2; 6, HS; 7, AsH_2; 8, SiH_3; 9, GeH_3; 10, HSe; 11,Cl; 12, Br) and E2 reactions (blue line, X = 1, HO; 2, F; 3, NH_2; 4, CH_3; 5, PH_2; 6, HS; 7, SiH_3; 8, AsH_2; 9, Cl; 10, GeH_3; 11, HSe; 12, Br) of X^- with EtCl along the increasing overall barrier trend.

3.5. Relationship of E2 and S_N2 Barrier Heights with Deformation Energy of the TS. In our previous papers,[35,36] it was found that there exist reasonable linear correlations between the deformation energies and overall barriers in the S_N2 and E2 reactions. Inspection of the data in Table 4 shows that the correlation only exists for the E2 reactions when the attacking atoms are on the same column in the periodic table, in which the deformation energies increase from top to bottom, whereas there is a linear correlation only for the group 17 Nus (halide anions) in the S_N2 reactions due to the irregular $n^{\ddagger}(C^{\alpha}-Cl)$ values when going down the groups 14−16. These results imply that the deformation energy does not generally dominate the overall barrier for both of the S_N2 and E2 reactions, and other factors need to be considered. Here, we use the idea of energy decomposition introduced by Bickelhaupt[67] to analyze the factors determining the barrier heights of S_N2 and E2 reactions, that is, the activation strain model. In this model, the overall reaction barrier can be partitioned into deformation energy (ΔH_{def}) and interaction (ΔH_{int}) between the deformed reactants in the TS. Figure 3 illustrates the variations of ΔH_{def} (normal line), ΔH_{int} (dashed line), and their sum, $\Delta H^{\ddagger}$ (bold line), for a series of E2 reactions (eq 1, blue line) and S_N2 reactions (eq 2, black line) along the increasing $\Delta H^{\ddagger}$ values. Generally speaking, a larger deformation energy will destabilize the TS and raise the overall barrier, but when the interaction between the deformed reactants is stronger, the barrier order could be reversed.

For the S_N2 reactions of the groups 14−16 Nus, the deformation energies from the second-row elements are slightly higher than those from the third-row ones by up to 7.2 kJ mol^{-1} induced by the longer $C^{\alpha}-Cl$ bond in the former cases. The overall barriers, $\Delta H^{\ddagger}(S_N2)$, are still increasing from top to bottom due to the stronger interaction between deformed reactants, which may be explained by the much higher ECA value of second-row Nus. Moreover, the interactions, ΔH_{int}, are found to correlate well with the ECAs in each column.

For all of the present E2 reactions, the deformation energies are in general much larger than the corresponding S_N2 reactions due to the fact that two bond cleavages are involved in the E2 TS, which has been also analyzed and pointed out by Bickelhaupt.[67] Meanwhile, the interactions between the deformed reactants in the E2 TS are also stronger than those in the S_N2 reactions except CH_3^- because of its larger PA value than the corresponding ECA one of X^-. For the CH_3^-case, the smaller ΔH_{int} value of −93.7 kJ mol^{-1} for the E2 TS, $[H_3C\cdots H^{\beta}\cdots CH_2CH_2\cdots Cl]^{-\ddagger}$, can be rationalized by the much smaller $n^{\ddagger}(C-H^{\beta})$ value, leading to weaker interaction between $CH_3^-$and H^{β} in the E2 TS.

3.6. Correlation of E2 and S_N2 Barrier Heights with Reaction Enthalpy. As shown in previous work,[68] the exothermicity of the reaction of nucleophile with a single substrate reflects the thermodynamic affinity of the nucleophile. Following this idea, the exothermicity trend, in this work, is given by the sequences of the overall enthalpy change, denoted as ΔH_{ovr}, as a function of Nu or base: the more negative is ΔH_{ovr}, the stronger is the exothermicity of the reaction. It can be seen from Table 4 that, for both the S_N2 and E2 reactions with substrate CH_3CH_2Cl, the exothermicity will decrease in going down a group, and the relationship between $\Delta H^{\ddagger}$ and ΔH_{ovr} follows the same trend as PA; that is, the consistency of the kinetics and thermodynamics for the present S_N2 and E2 reactions only exists within each column of the periodic table.

3.7. Competition between S_N2 and E2 Reactions. Comparison of the E2 and S_N2 overall barriers in Table 4 shows that the S_N2 pathway is much more favorable for all of the second- and third-row Nus, which is consistent with previous results. For the first-row bases, E2 dominates for reactions of $F^- + CH_3CH_2Cl$ and $HO^- + CH_3CH_2Cl$, and S_N2 and E2 pathways are competitive for the reaction of $NH_2^- + CH_3CH_2Cl$, whereas S_N2 reaction dominates for $CH_3^- + CH_3CH_2Cl$.

If we combine the correlations between S_N2 and E2 overall barriers and PA values along each column of periodical table, a very clear picture emerges from the analysis of the crossing points. Figure 2 shows that the crossing points from the two series of correlations of $\Delta H^{\ddagger}$ versus PA of X will shift to the right from group 17 to group 14, which implies that the favorable pathway is related to the position of the attacking atom in the periodic table.

4. Conclusions

This work systematically studies the reactions of ethyl chloride with a series of Nus covering the groups 14−17 elements using the G2(+) method. Two competitive reaction pathways, back-side S_N2 and *anti*-E2, are investigated, leading to the following conclusions.

(1) For both the S_N2 and the E2 reactions, the good correlation between G2(+) PAs and overall barriers, $\Delta H^{\ddagger}$, only exists when the attacking atoms belong to the same group in the periodic table. This modifies the previous claim

that $\Delta H^{\ddagger}$ values for the S_N2 and E2 reactions are basically controlled by the PA of bases. Thus, it is more reasonable to make a reference line using the nucleophiles or bases with the attacking atom in the same group when discussing the α-effect in the E2 and S_N2 reactions.

(2) A strong correlation is found between the EN of the attacking atom and the barrier heights of S_N2 and E2 reactions. A higher EN value of X will stabilize the S_N2 and E2 TS by less electron reorganization. Good linear correlation exists for $\Delta H^{\ddagger}$ versus EN within the same column of the periodic table.

(3) Two-parameter equations are derived to connect the S_N2 or E2 overall barriers with the combination of PA and EN values of the attacking atom by multiple linear regression analysis, indicating the importance of both PA and EN in determining the S_N2 or E2 reactivity. Thus, the PA and EN values may be used to predict the overall barrier of the S_N2 or E2 reactions involving normal Nu.

(4) It is found that the good correlation of $\Delta H^{\ddagger}$ versus ΔH_{def} only exists in E2 reactions with attacking atoms in the same group, which deviates from the previous conclusion that there is a general linear relationship between the overall barrier and all Nus or bases.

Acknowledgment. This work is supported by a Strategic Grant (Project No. 7002334) from the City University of Hong Kong.

Supporting Information Available: Cartesian coordinates of all species reported. This material is available free of charge via the Internet at http://pubs.acs.org.

References

(1) Lowry, T. H.; Richardson, K. S. *Mechanism and Theory in Organic Chemistry*, 3rd ed.; Harper and Row: New York, 1987.

(2) Jones, M. E.; Ellison, G. B. *J. Am. Chem. Soc.* **1989**, *111*, 1645.

(3) Dhar, M. L.; Hughes, E. D.; Ingold, C. K.; Masterman, S. *J. Chem. Soc.* **1948**, *48*, 2055.

(4) Lum, R. C.; Grabowski, J. J. *J. Am. Chem. Soc.* **1992**, *114*, 9663.

(5) Flores, A. E.; Gronert, S. *J. Am. Chem. Soc.* **1999**, *121*, 2627.

(6) Gronert, S.; Fagin, A. E.; Okamoto, K.; Mogali, S.; Pratt, L. M. *J. Am. Chem. Soc.* **2004**, *126*, 12977.

(7) Gronert, S.; Fagin, A. E.; Wong, L. *J. Am. Chem. Soc.* **2007**, *17*, 5331.

(8) DePuy, C. H.; Bierbaum, V. M. *J. Am. Chem. Soc.* **1981**, *103*, 5034.

(9) DePuy, C. H.; Beedle, E. C.; Bierbaum, V. M. *J. Am. Chem. Soc.* **1982**, *104*, 6483.

(10) DePuy, C. H.; Gronert, S.; Mullin, A.; Bierbaum, V. M. *J. Am. Chem. Soc.* **1990**, *112*, 8650.

(11) Gronert, S.; DePuy, C. H.; Bierbaum, V. M.; DePuy, C. H. *J. Am. Chem. Soc.* **1991**, *113*, 4009.

(12) Ridge, D. P.; Beauchamp, J. L. *J. Am. Chem. Soc.* **1974**, *96*, 637.

(13) Minato, T.; Yamabe, S. *J. Am. Chem. Soc.* **1980**, *107*, 4621.

(14) Bento, A. P.; Solà, M.; Bickelhaupt, F. M. *J. Chem. Theory Comput.* **2008**, *4*, 929.

(15) Gronert, S.; Merrill, G. N.; Kass, S. R. *J. Org. Chem.* **1995**, *60*, 488.

(16) Gronert, S. *J. Am. Chem. Soc.* **1991**, *113*, 6041.

(17) Gronert, S. *J. Am. Chem. Soc.* **1993**, *115*, 652.

(18) Gronert, S.; Kass, S. R. *J. Org. Chem.* **1997**, *62*, 7991.

(19) Gronert, S. *J. Org. Chem.* **1994**, *59*, 7046.

(20) Gronert, S.; Freed, P. *J. Org. Chem.* **1996**, *61*, 9430.

(21) Hu, W.-P.; Truhlar, D. G. *J. Am. Chem. Soc.* **1996**, *118*, 860.

(22) Villano, S. M.; Kato, S.; Bierbaum, V. M. *J. Am. Chem. Soc.* **2006**, *128*, 736.

(23) Su, T.; Chesnavich, W. J. *J. Chem. Phys.* **1982**, *76*, 5183.

(24) Pabis, A.; Paluch, P.; Szala, J.; Paneth, P. *J. Chem. Theory Comput.* **2009**, *5*, 33.

(25) Zhao, Y.; Schultz, N. E.; Truhlar, D. G. *J. Chem. Theory Comput.* **2006**, *2*, 364.

(26) Zhao, Y.; Truhlar, D. G. *Theor. Chem. Acc.* **2008**, *120*, 215; Erratum: *Theor. Chem. Acc.* **2008**, *119*, 525.

(27) Miertus, S.; Scrocco, E.; Tomasi, J. *J. Chem. Phys.* **1981**, *55*, 117.

(28) Glukhovtsev, M. N.; Pross, A.; Radom, L. *J. Am. Chem. Soc.* **1995**, *117*, 2024.

(29) Glukhovtsev, M. N.; Pross, A.; Radom, L. *J. Am. Chem. Soc.* **1995**, *117*, 9012.

(30) Bento, A. P.; Bickelhaupt, F. M. *J. Org. Chem.* **2008**, *73*, 7290.

(31) Lee, I.; Kim, C. K.; Lee, B. S. *J. Phys. Org. Chem.* **1995**, *8*, 473.

(32) Uggerud, E. *Chem.-Eur. J.* **2006**, *12*, 1127.

(33) Glukhovtsev, M. N.; Pross, A.; Radom, L. *J. Am. Chem. Soc.* **1996**, *118*, 6273.

(34) Ren, Y.; Yamataka, H. *Org. Lett.* **2006**, *8*, 119.

(35) Ren, Y.; Yamataka, H. *J. Org. Chem.* **2007**, *72*, 5660.

(36) Ren, Y.; Yamataka, H. *J. Comput. Chem.* **2009**, *30*, 358.

(37) Bento, A. P.; Sola, M.; Bickelhaupt, F. M. *J. Comput. Chem.* **2005**, *26*, 1497.

(38) Mourik, T. v. *Chem. Phys. Lett.* **2005**, *414*, 364.

(39) Reed, A. E.; Curtiss, L. A.; Weinhold, F. *Chem. Rev.* **1988**, *88*, 899.

(40) Houk, K. N.; Gustafson, S. M.; Black, K. A. *J. Am. Chem. Soc.* **1992**, *114*, 8565.

(41) Lee, J. K.; Kim, C. K.; Lee, B. S.; Lee, I. *J. Phys. Chem. A* **1997**, *101*, 2893.

(42) Kim, C. K.; Hyun, K. H.; Kim, C. K.; Lee, I. *J. Am. Chem. Soc.* **2000**, *122*, 2294.

(43) Frisch, M. J.; Trucks, G. W.; Schlegel, H. B.; Scuseria, G. E.; Robb, M. A.; Cheeseman, J. R.; Montgomery, J. A., Jr.; Vreven, T.; Kudin, K. N.; Burant, J. C.; Millam, J. M.; Iyengar, S. S.; Tomasi, J.; Barone, V.; Mennucci, B.; Cossi, M.; Scalmani, G.; Rega, N.; Petersson, G. A.; Nakatsuji, H.; Hada, M.; Ehara, M.; Toyota, K.; Fukuda, R.; Hasegawa, J.; Ishida, M.; Nakajima, T.; Honda, Y.; Kitao, O.; Nakai, H.; Klene, M.; Li, X.; Knox, J. E.; Hratchian, H. P.; Cross, J. B.; Bakken, V.; Adamo, C.; Jaramillo, J.; Gromperts, R.; Strat-

mann, R. E.; Yazyev, O.; Austin, A. J.; Cammi, R.; Pomelli, C.; Ochterski, J. W.; Ayala, P. Y.; Morokuma, K.; Voth, G. A.; Salvador, P.; Dannenberg, J. J.; Zakrzewski, G.; Dapprich, S.; Daniels, A. D.; Strain, M. C.; Farkas, O.; Malick, D. K.; Rabuck, A. D.; Raghavachari, K.; Foresman, J. B.; Ortiz, J. V.; Cui, Q.; Baboul, A. G.; Clifford, S.; Cioslowski, J.; Stefanov, B. B.; Liu, G.; Liashenko, A.; Piskorz, P.; Komaromi, I.; Martin, R. L.; Fox, D. J.; Keith, T.; Al-Laham, M. A.; Peng, C. Y.; Nanayakkara, A.; Challacombe, M.; Gill, P. M. W.; Johnson, B.; Cheng, W.; Wong, M. W.; Gonzalez, C.; Pople, J. A. *Gaussian 03*, revision D.01; Gaussian, Inc.: Pittsburgh, PA, 2003; Wallingford, CT, 2004.

(44) NIST Standard reference Database Number 69; http:/webbook.nist.gov/chemistry (accessed Jan 22, 2009).

(45) Decouzon, M.; Gal, J. F.; Gayraud, J.; Maria, P. C.; Vaglio, G. A.; Volpe, P. *J. Am. Soc. Mass Spectrom.* **1993**, *4*, 54.

(46) Ervin, K. E.; Lineberger, C. W. *J. Chem. Phys.* **2005**, *122*, 194303.

(47) Mayer, P. M.; Gal, J. F.; Radom, L. *Int. J. Mass Spectrom. Ion Processes* **1997**, *167*−*168*, 689.

(48) Bartmess, J. E.; Hinde, R. J. *Can. J. Chem.* **2005**, *83*, 2005.

(49) Lischka, H.; Köhler, H. J. *J. Am. Chem. Soc.* **1978**, *100*, 5297.

(50) Raghavachari, K.; Whiteside, R. A.; Pople, J. A.; Schleyer, P. v. R. *J. Am. Chem. Soc.* **1981**, *103*, 5649.

(51) Ruscic, B.; Berkowitz, J.; Curtiss, L. A.; Pople, J. A. *J. Chem. Phys.* **1989**, *91*, 114.

(52) Klopper, W.; Kutzelnigg, W. *J. Phys. Chem.* **1990**, *94*, 5625.

(53) Carneiro, J. W.; de, M.; Schleyer, P. v. R.; Saunders, M.; Remington, R.; Schaefer, H. F., III; Rauk, A.; Sorensen, T. S. *J. Am. Chem. Soc.* **1994**, *116*, 3483.

(54) Perera, S. A.; Bartlett, J.; Schleyer, P. v. R. *J. Am. Chem. Soc.* **1995**, *117*, 8476.

(55) Rio, E. Del.; Lopez, R.; Sordo, T. L. *J. Phys. Chem. A* **1998**, *102*, 6831.

(56) Andrei, H. S.; Solcà, N.; Dopfer, O. *Angew. Chem., Int. Ed.* **2008**, *47*, 395.

(57) Nibbering, N. M. M. *Acc. Chem. Res.* **1990**, *23*, 279.

(58) Nibbering, N. M. M. *Adv. Phys. Org. Chem.* **1988**, *24*, 1.

(59) Bierbaurn, V. M.; Grabowski, J. J.; DePuy, C. H. *J. Phys. Chem.* **1984**, *88*, 1389.

(60) Anderson, D. R.; Bierbaum, V. M.; DePuy, C. H. *J. Am. Chem. Soc.* **1983**, *105*, 4244.

(61) Gronert, S. *J. Am. Chem. Soc.* **1993**, *115*, 10258.

(62) Luo, Y. R.; Benson, S. W. *J. Am. Chem. Soc.* **1989**, *111*, 2480.

(63) Winter, M. J. The periodic table on the WWW; http://www.webelements.com, Copyright 1993−2009.

(64) Pierrefixe, S. C. A. H.; Guerra, C. F.; Bickelhaupt, F. M. *Chem.-Eur. J.* **2008**, *14*, 819.

(65) Pierrefixe, S. C. A. H.; Poater, J.; Im, C.; Bickelhaupt, F. M. *Chem.-Eur. J.* **2008**, *14*, 6901.

(66) Pierrefixe, S. C. A. H.; Bickelhaupt, F. M. *Struct. Chem.* **2007**, *18*, 813.

(67) Bickelhaupt, F. M. *J. Comput. Chem.* **1999**, *20*, 114.

(68) Olmstead, W. N.; Brauman, J. I. *J. Am. Chem. Soc.* **1977**, *99*, 4219.

CT900041Y